Electrochemical Studies of Rhodium-Carbon Bond Formation. The Reaction of Monomeric (Tetraphenylporphinato)rhodium(II) with Alkyl and Aryl Halides

J. E. Anderson, C.-L. Yao, and K. M. Kadish*

Contribution from the Department of Chemistry, University of Houston, Houston, Texas 77004.
Received July 29, 1986

Abstract: The reaction of electrochemically generated (TPP)Rh (where TPP is the dianion of tetraphenylporphyrin) with 24 different alkyl or aryl halides (RX) was monitored by electrochemical and spectroelectrochemical methods. (TPP)Rh was generated by the one-electron reduction of $[(TPP)Rh(L)_2]^+Cl^-$, where L is dimethylamine. The reduced rhodium complex reacts with alkyl halides in solution to form (TPP)Rh(R) and X^-, and the synthesis of 14 different (TPP)Rh(R) complexes by this method is reported. However, no reaction between (TPP)Rh and aryl halides is observed. Relative reaction rate constants for the reaction between (TPP)Rh and the alkyl halides were evaluated as a function both the halide, X, and the R group of the alkyl halide. In general, the dependence of the reaction rate constants on the halide followed the trend I > Br > F ≥ Cl, while the dependence of the reaction rate constants on R of the straight chain isomers followed the trend $CH_3 > C_2H_5 \approx C_3H_7 \approx C_4H_9 \approx C_5H_{11}$. On the basis of these results, a general discussion of the reaction mechanism for the formation of (TPP)Rh(R) from (TPP)Rh and RX is presented.

Monomeric (TPP)Rh can be generated by the one electron reduction of $[(TPP)Rh(L)_2]^+Cl^-$ where TPP is the dianion of tetraphenylporphyrin and L is dimethylamine.[1] The electrogenerated (TPP)Rh can either dimerize,[1] or it can react to form a rhodium-carbon σ bonded species.[2] The reactions of $[(P)Rh]_2$ (where P is the dianion of a porphyrin macrocycle) with alkyl halides,[3,4] alkenes,[3-5] alkynes,[3,4] and alkylaromatics[6,7] also result in formation of a rhodium-carbon σ bonded species.

In general, rhodium macrocycles form metal-carbon bonds by either a two-electron S_N2-like mechanism[8,9] or by a radical one-electron process.[8,10,11] Kinetic studies for the reaction of $[(P)Rh]_2$ with alkenes demonstrate a free-radical process.[12] The first step in this reaction is the dissociation of $[(P)Rh]_2$ to form (P)Rh. Formation of (P)Rh has also been reported in other studies.[1,2,6,7,13,14] This reactive monomeric Rh(II) species has never been isolated, but its optical spectrum has been measured at 77 K.[14]

Reactivity studies of rhodium(II) porphyrins are based primarily on data of $[(P)Rh]_2$. Hence, there is the initial requirement that the $[(P)Rh]_2$ dimer must dissociate. This equilibrium favors dimeric $[(P)Rh]_2$ over monomeric (P)Rh and thus results in reactions which occur only at long times and/or elevated temperatures.[4,6,7] One consequence of this is that much information about the reactivity of monomeric (P)Rh is lost.

The reactivity of electrochemically generated (P)Rh should be the same as that observed by chemical generation from $[(P)Rh]_2$, but in the case of electrochemical generation, much higher concentrations of the reactive species can be observed at the electrode surface. In addition, electrochemical techniques have the distinct advantage that the technique can be used to monitor the homogeneous reactions of electrogenerated species as well as any electroactive species formed by reactions involving these electrogenerated complexes. This is illustrated in the present paper which examines the chemical reactivity of (TPP)Rh with 24 different alkyl or aryl halides. The halide and the R group in RX were systematically varied, and the effect of X and R on relative reaction rate constants was examined by electrochemical methods. The electrochemically initiated synthesis of 14 different (P)Rh(R) compounds is reported, and on the basis of the electrochemical and reactivity data the mechanism for the reaction of (TPP)Rh and RX is discussed.

Experimental Section

Materials. Spectroscopic grade tetrahydrofuran (THF) was purchased from Aldrich and purified by distillation under nitrogen first from CaH_2 and then from sodium/benzophenone just prior to use. Spectroscopic grade benzene (C_6H_6) was purchased from Aldrich, purified by distillation under nitrogen from sodium. Tetra-*n*-butylammonium perchlorate (TBAP) was purchased from Fluka Chemical Co., twice recrystallized from ethyl alcohol, and dried in a vacuum oven at 40 °C. All organic reagents (Aldrich) were purchased at the highest level of purity available, purified by standard procedures[15] where necessary, and checked for impurities by gas chromatographic analysis prior to use. Deuteriated benzene-d_6 (C_6D_6) was purchased from Aldrich and used without further purification. The rhodium-porphyrin complex $[(TPP)Rh(L)_2]^+Cl^-$ where L is dimethylamine $[NH(CH_3)_2]$ was synthesized by methods already in the literature.[1,16]

Instrumentation and Methods. An IBM 225/2A voltammetric analyzer coupled with a Houston Instruments Model 2000 X-Y recorder was used for cyclic voltammetric and polarographic measurements. All electrochemical measurements and bulk electrolysis experiments, with the exception of thin-layer spectroelectrochemistry, were performed in cells modified for Schlenk techniques. Platinum disk electrodes were used, except in the thin-layer spectroelectrochemical cell and the bulk electrolysis cell where platinum minigrid electrodes were used. The thin-layer spectroelectrochemical cell has been previously described.[17] Thin-layer spectroelectrochemical measurements were made with an IBM 225/2A voltammetric analyzer coupled with a Tracor Northern 1710 spectrometer/multichannel analyzer. Bulk controlled potential coulometry was

(1) Kadish, K. M.; Yao, C.-L.; Anderson, J. E.; Cocolios, P. *Inorg. Chem.* **1985**, *24*, 4515.
(2) Anderson, J. E.; Yao, C.-L.; Kadish, K. M. *Inorg. Chem.* **1986**, *25*, 718.
(3) Ogoshi, H.; Setsune, J.; Yoshida, Z. *J. Am Chem. Soc.* **1977**, *99*, 3869.
(4) Setsune, J.; Yoshida, Z.; Ogoshi, H. *J. Chem. Soc., Perkin Trans. 1* **1982**, 983.
(5) Ogoshi, H.; Setsune, J.; Nanbo, Y.; Yoshida, Z. *J. Chem. Soc., Perkin Trans. 1* **1980**, 1641.
(6) Wayland, B. B.; Del Rossi, K. *J. Organomet. Chem.* **1984**, *276*, C27.
(7) Del Rossi, K.; Wayland, B. B. *J. Am. Chem. Soc.* **1985**, *107*, 7941.
(8) Hughes, R. P. *Comprehensive Organometallic Chemistry*; Wilkinson, G., Ed.; Pergamon Press: New York, 1982; Vol. 5, p 277.
(9) Collman, J. P.; Brauman, J. I.; Madonik, A. M. *Organometallics* **1986**, *5*, 310.
(10) Collman, J. P.; Brauman, J. I.; Madonik, A. M. *Organometallics* **1986**, *5*, 215.
(11) Collman, J. P.; Brauman, J. I.; Madonik, A. M. *Organometallics* **1986**, *5*, 218.
(12) Paonessa, R. S.; Thomas, N. C.; Halpern, J. *J. Am. Chem. Soc.* **1985**, *107*, 4333.
(13) Van Voorhees, S.; Wayland, B. B. *Organometallics* **1985**, *4*, 1887.
(14) Hoshino, M.; Yasufuku, K.; Konishi, S.; Imamura, M. *Inorg. Chem.* **1984**, *23*, 1982.
(15) Perrin, D. D.; Armarego, W. L. F.; Perrin, D. R. *Purification of Laboratory Chemicals*, 2nd ed.; Pergamon Press: New York, 1980.
(16) Fleischer, E. B.; Dixon, F. L.; Florian, R. *Inorg. Nucl. Chem. Lett.* **1973**, *9*, 1303.
(17) Lin, X.-Q.; Kadish, K. M. *Anal. Chem.* **1985**, *57*, 1498.

0002-7863/87/1509-1106$01.50/0

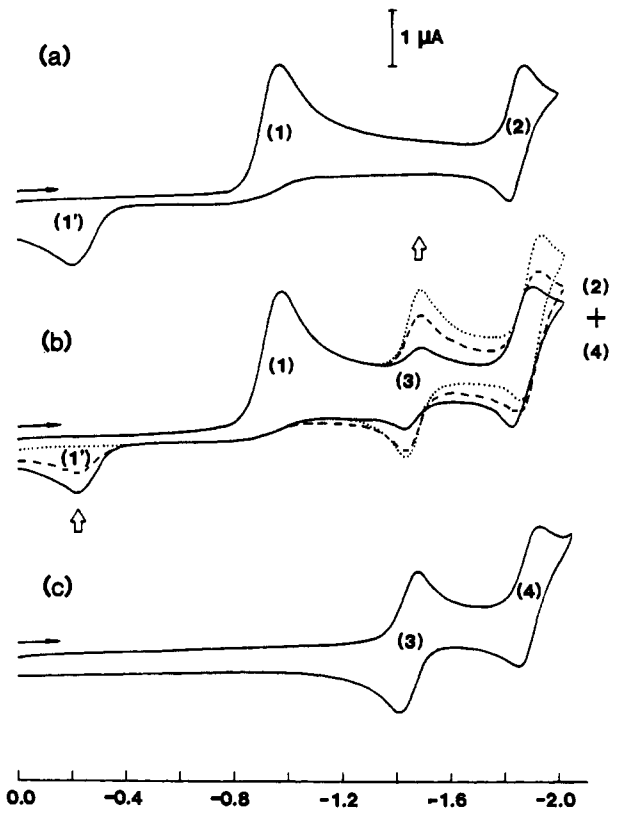

Figure 1. Cyclic voltammograms of 9.9×10^{-4} M $[(TPP)Rh(L)_2]^+Cl^-$ in the presence of (a) 0 equiv of CH_3I; (b) 0.1 (—), 0.3 (– – –), and 1.0 (···) equiv of CH_3I; and (c) cyclic voltammogram of $(TPP)Rh(CH_3)$. The solvent was THF, 0.2 M TBAP. Scan rate = 100 mV/s.

performed on an EG&G Princeton Applied Research Model 174 potentiostat/179 coulometer system coupled with an EG&G Princeton Applied Research Model RE-0074 time base X-Y recorder. Potentials were measured vs. a saturated calomel electrode (SCE) which was separated from the bulk of the solution by a fritted-glass disk junction. Ferrocene was used as an internal standard against which potentials were also measured. Unless otherwise noted, 0.2 M tetrabutylammonium perchlorate (TBAP) was used as supporting electrolyte for cyclic voltammetric measurements, bulk solution electrolysis, and spectroelectrochemical measurements.

Syntheses of the (TPP)Rh(R) complexes were performed under an inert atmosphere by Schlenk techniques as follows: $[(TPP)Rh(L)_2]^+Cl^-$ (10–20 mg) and 10–20 equiv of RX were dissolved in THF, 0.2 TBAP. Bulk electrolysis at −1.2 V was performed with the monitoring of the current time curve. After complete electrolysis, the number of electrons were calculated, and the solution was transferred from the bulk electrolysis cell to another flask, followed by isolation procedures. In general, the (TPP)Rh(R) complexes were isolated by first evaporating the solution to dryness and extracting with benzene at 10 °C, followed by purification on an alumina column. For the complexes $(TPP)Rh(C_nH_{2n+1})$, n = 1, 2, 3, 4, and 5, the percent yields were nearly quantitative (≥90%), while for the other complexes the percent yields ranged from 50% to 90%.

UV–vis spectra were recorded either on the Tracor Northern 1710 spectrometer/multichannel analyzer or with an IBM 9430 spectrophotometer by using cells adapted for inert atmosphere measurements. NMR spectra were taken on a Nicolet FT 300 spectrometer. Gas chromatographic analysis was performed with a Hewlett-Packard 5890 gas chromatograph coupled with a Hewlett-Packard 3392A integrator. One of two packed columns, a 6-ft, 3% OV-1 on 100/120 chromosorb or a 10-ft, 10% TCEP on 100/120 chromosorb was used with an FID detector. The carrier gas was nitrogen. The various flow rates and temperature profiles were optimized for the particular column and sample used.

Results and Discussion

Reaction of (TPP)Rh with RX. The reaction of (TPP)Rh with various alkyl or aryl halides was monitored by cyclic voltammetry. The method is demonstrated in Figure 1a,b. These figures show

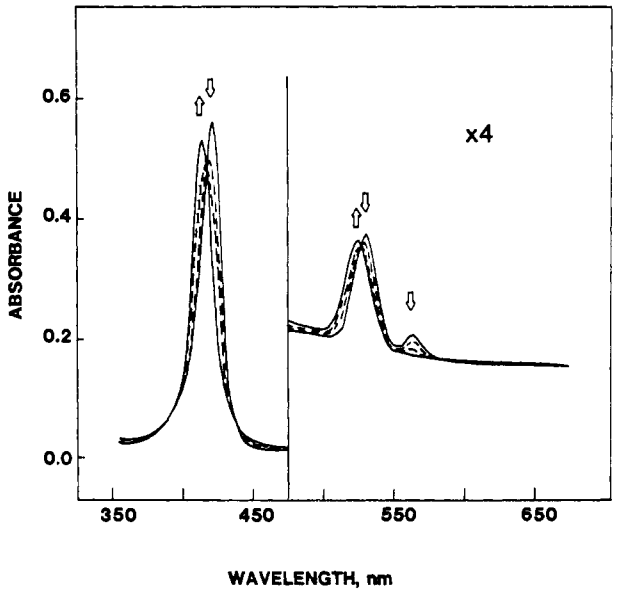

Figure 2. Electronic absorption spectra for the reduction of 8.3×10^{-5} M $[(TPP)Rh(L)_2]^+Cl^-$ in THF/0.2 M TBAP at −1.20 V in the presence of 10 equiv of CH_3I.

cyclic voltammograms of $[(TPP)Rh(L)_2]^+Cl^-$ in THF containing various amounts of CH_3I. In the absence of CH_3I there are three major electrode processes. These are an irreversible reduction wave at E_p = −0.92 V (wave 1, Figure 1a), a reversible reduction/reoxidation wave at $E_{1/2}$ = −1.83 V (wave 2, Figure 1a), and an irreversible oxidation wave at E_p = −0.22 V (wave 1′, Figure 1a).[18] The first process (wave 1) is due to the irreversible, one-electron reduction of $[(TPP)Rh(L)_2]^+Cl^-$ and results in the electrochemical generation of (TPP)Rh. This electrode reaction is followed by dimerization of (TPP)Rh to give $[(TPP)Rh]_2$. The reversible process at $E_{1/2}$ = −1.83 V is the two-electron reduction of $[(TPP)Rh]_2$ while the process at E_p = −0.22 V is due to the oxidation of this dimeric species.[1]

Figure 1b shows the changes that occur in the cyclic voltammogram of $[(TPP)Rh(L)_2]^+Cl^-$ as CH_3I is added to the solution. The first irreversible reduction remains unchanged, while a new reversible process at $E_{1/2}$ = −1.44 V (process 3, Figure 1b) progressively increases in current. At the same time, the oxidation at E_p = −0.22 V decreases in current, and the reduction at $E_{1/2}$ = −1.83 V which is associated with $[(TPP)Rh]_2$ appears to shift to more negative potentials. However, this apparent shift is actually due to an overlap of the process at −1.83 V with a new process 4 that occurs at −1.88 V (see Figure 1c). The cyclic voltammogram continues to change up to the addition of 1 equiv of CH_3I after which no further changes are observed. The final voltammogram is characterized by the three one-electron reductions at E_p = −0.92 V, $E_{1/2}$ = −1.44 V, and $E_{1/2}$ = −1.88 V.

The new reversible reductions in Figure 1b are due to the stepwise reduction of $(TPP)Rh(CH_3)$ at $E_{1/2}$ = −1.44 and −1.88 V. This was verified by experiments carried out on authentic samples of $(TPP)Rh(CH_3)$ which were prepared by chemical methods.[19] A cyclic voltammogram of $(TPP)Rh(CH_3)$ is shown in Figure 1c. Complexes of the type (TPP)Rh(R) typically have two reduction waves whose potentials are close to those observed for $(TPP)Rh(CH_3)$.[20]

The electronic absorption spectra also demonstrate formation of $(TPP)Rh(CH_3)$ upon electroreduction of $[(TPP)Rh(L)_2]^+Cl^-$ in the presence of CH_3I. This is shown in Figure 2. The electronic

(18) Corresponding peaks are reported in benzonitrile at a scan rate of 100 mV/s. The wave at E_p = −1.06 is a one-electron, diffusion-controlled process, while the wave at $E_{1/2}$ = −1.95 V is a diffusion-controlled two-electron process. For full characterization of these waves see ref 1.

(19) Ogoshi, H.; Omura, T.; Yoshida, Z. *J. Am. Chem. Soc.* **1973**, *95*, 1666.

(20) Kadish, K. M.; Anderson, J. E.; Yao, C.-L.; Guilard, R. *Inorg. Chem.* **1986**, *25*, 1277.

Table I. A List of Alkyl Halides (RX) Used in This Study and the UV–vis Spectra and Reduction Potentials for the Electrogenerated (TPP)Rh(R) Complexes in THF[c]

	RX	electrogenerated porphyrin	$E_{1/2}$ (V vs. SCE)[a]	λ (ε × 10^{-3})		
		$[(TPP)Rh(L)_2]^+Cl^-$		418 (253)	529 (23.7)	562 (5.0)
(1)	CH_2Cl_2	$(TPP)Rh(CH_2Cl)$	−1.42	415 (200)	527 (19.7)	
(2)	$CHCl_3$	$(TPP)Rh(CHCl_2)$	−1.41	418 (208)	529 (21.8)	
(3)	CCl_4	$(TPP)Rh(CCl_3)$	−1.41	421 (212)	533 (20.6)	
(4)	CH_2Br_2	$(TPP)Rh(CH_2Br)$	−1.43	413 (219)	526 (22.4)	
(5)	CH_2I_2	$(TPP)Rh(CH_2I)$	−1.43	415 (185)	527 (17.6)	
(6)	CHI_3	$(TPP)Rh(CHI_2)$	−1.43	418 (155)	528 (20.2)	
(7)	CI_4	$(TPP)Rh(CI_3)$	−1.43	416 (118)	526 (16.7)	
(8)	CH_3I	$(TPP)Rh(CH_3)$	−1.44	412 (240)	524 (22.5)	
(9)	CH_3CH_2I	$(TPP)Rh(CH_2CH_3)$	−1.42	410 (235)	524 (20.8)	
(10)	CH_3CH_2Br	$(TPP)Rh(CH_2CH_3)$	−1.42	410 (235)	524 (20.8)	
(11)	$CH_3CH_2CH_2I$	$(TPP)Rh(CH_2CH_2CH_3)$	−1.42	411 (209)	525 (19.6)	
(12)	$CH_3CH_2CH_2Br$	$(TPP)Rh(CH_2CH_2CH_3)$	−1.42	411 (209)	525 (19.6)	
(13)	$CH_3CH_2CH_2CH_2I$	$(TPP)Rh(CH_2CH_2CH_2CH_3)$	−1.42	411 (235)	525 (20.7)	
(14)	$CH_3CH_2CH_2CH_2Br$	$(TPP)Rh(CH_2CH_2CH_2CH_3)$	−1.42	411 (235)	525 (20.7)	
(15)	$CH_3CH_2CH_2CH_2Cl$	$(TPP)Rh(CH_2CH_2CH_2CH_3)$	−1.42	411 (235)	525 (20.7)	
(16)	$CH_3CH_2CH_2CH_2CH_2I$	$(TPP)Rh(CH_2CH_2CH_2CH_2CH_3)$	−1.42	411 (227)	523 (19.5)	
(17)	$CH_3CH_2CH_2CH_2CH_2Br$	$(TPP)Rh(CH_2CH_2CH_2CH_2CH_3)$	−1.42	411 (227)	523 (19.5)	
(18)	$CH_3CH_2CH_2CH_2CH_2Cl$	$(TPP)Rh(CH_2CH_2CH_2CH_2CH_3)$	−1.42	411 (227)	523 (19.5)	
(19)	$CH_3CH_2CH_2CH_2CH_2F$	$(TPP)Rh(CH_2CH_2CH_2CH_2CH_3)$	−1.42	411 (227)	523 (19.5)	
(20)	$CH_3CH_2CH(CH_3)Cl$	$(TPP)Rh(CH(CH_3)CH_2CH_3)$[b]		417	530	
(21)	$(CH_3)_3CCl$	$(TPP)Rh(C(CH_3)_3)$[b]		415		
(22)	C_6H_5I	no reaction				
(23)	C_6H_5Br	no reaction				
(24)	C_6H_5Cl	no reaction				

[a] Wave 3. [b] Complete formation of (P)Rh(R) is not observed. Spectra are uncertain due to the presence of $[(P)Rh]_2$. [c] 0.2 M TBAP.

Table II. ^1H NMR Data of Electrochemically Generated (TPP)Rh(R) Complexes[a]

electrogenrtd porphyrin, (TPP)Rh(R)	TPP resonances			R	J_{Rh-H} (H_2)
	pyr H	phenyl H	phenyl H		
$(TPP)Rh(CH_2Cl)$[b]	8.99 (8 H, s)	8.29 (8 H, m)	7.76 (12 H, m)	−2.81 (2 H, d)	2.9
$(TPP)Rh(CH_3)$[c]	8.85 (8 H, s)	8.14 (8 H, m)	7.45 (12 H, m)	−5.54 (3 H, d)	4.5
$(TPP)Rh[(CH_2)_2CH_3]$[c]	8.86 (8 H, s)	8.18 (8 H, m)	7.46 (12 H, m)	−4.65 (2 H, m) −4.11 (2 H, m) −1.78 (3 H, t)	2.4
$(TPP)Rh[(CH_2)_3CH_3]$	8.89 (8 H, s)	8.20 (8 H, m)	7.48 (12 H, m)	−4.62 (2 H, m) −4.17 (2 H, m) −1.57 (2 H, m) −0.81 (3 H, t)	2.6
$(TPP)Rh[(CH_2)_4CH_3]$[c]	8.86 (8 H, s)	8.19 (8 H, m)	7.47 (12 H, m)	−4.62 (2 H, m) −4.18 (2 H, m) −1.61 (2 H, m) −0.50 (2 H, m) −0.27 (3 H, t)	2.4

[a] All resonances reported relative to Me_4Si. [b] Pyridine-d_5 as solvent, see ref 2. [c] C_6D_6 as solvent.

absorption spectrum of $[(TPP)Rh]_2$ is characterized by bands at 404 and 496 nm.[1] However, in the presence of CH_3I, the first one-electron reduction of $[(TPP)Rh(L)_2]^+Cl^-$ at −1.20 V has a product whose spectrum is characterized by bands at 412 and 524 nm. This spectrum is identical with one obtained for authentic samples of $(TPP)Rh(CH_3)$ under similar solution conditions.

^1H NMR spectra were taken for the product isolated after bulk electrolysis of $[(TPP)Rh(L)_2]^+Cl^-$ at −1.20 V in the presence of CH_3I and are also consistent with formation of $(TPP)Rh(CH_3)$. Porphyrin signals are located at 8.85 (pyr H, s, 8 H), 8.14 (phenyl H, m, 8 H), and 7.45 ppm (phenyl H, m, 12 H), all relative to Me_4Si. A doublet at −5.54 ppm (3 H) is observed and is due to the Rh–CH_3 signal. The J_{Rh-H} coupling is 4.5 Hz which is similar to that reported for $(OEP)Rh(CH_3)$.[21]

Electrogenerated (TPP)Rh is unstable, and two reaction pathways are available to (TPP)Rh when CH_3I is present in solution. The first pathway involves a reaction with CH_3I to produce $(TPP)Rh(CH_3)$, while the second pathway involves dimerization of (TPP)Rh to form $[(TPP)Rh]_2$. It is clear from Figure 1 that the first reaction pathway predominates and that $(TPP)Rh(CH_3)$ is the major product in solutions containing CH_3I.

The electrochemical generation of $(TPP)Rh(CH_2Cl)$ and $(TPP)Rh(CH_3)$ has been demonstrated for the reaction of (TPP)Rh with CH_2Cl_2 and CH_3I, respectively. The formation of (TPP)Rh(R) occurs for 21 of the 24 RX compounds investigated in this study (see list of RX in Table I). This conclusion is based on both the UV–vis spectra of the products and the cyclic voltammograms of $[(TPP)Rh(L)_2]^+$ in the presence of RX. In addition to (TPP)Rh(R) formation of X^- is also observed. Formation of X^- during bulk electrolysis and a mechanistic evaluation of this reaction are presented in a later section of this manuscript.

Reports of (TPP)Rh(R) formation from alkyl halides[3,4] are in agreement with results in this present study. Electrochemical generation of 14 different (TPP)Rh(R) compounds was possible, and Table I presents the spectral and electrochemical data of the final products. Figure 3 presents the ^1H NMR spectrum from 0 to −6 ppm for $(TPP)Rh(C_3H_7)$ and $(TPP)Rh(C_5H_{11})$, isolated from reaction of electrogenerated (TPP)Rh with C_3H_7I and $C_5H_{11}I$. The ^1H NMR unambigiously demonstrates the identity of the R group of the (TPP)Rh(R) products. Table II lists the complete ^1H NMR data for five of the isolated (TPP)Rh(R) compounds.

The aryl halides C_6H_5X where X = Cl, Br, or I do not react with (TPP)Rh. The fact that these compounds do not react with (TPP)Rh may seem surprising since $(P)Rh(CH_2C_6H_5)$ and

(21) Ogoshi, H.; Setsune, J.; Omura, T.; Yoshida, Z. *J. Am Chem. Soc.* **1975**, *97*, 6461.

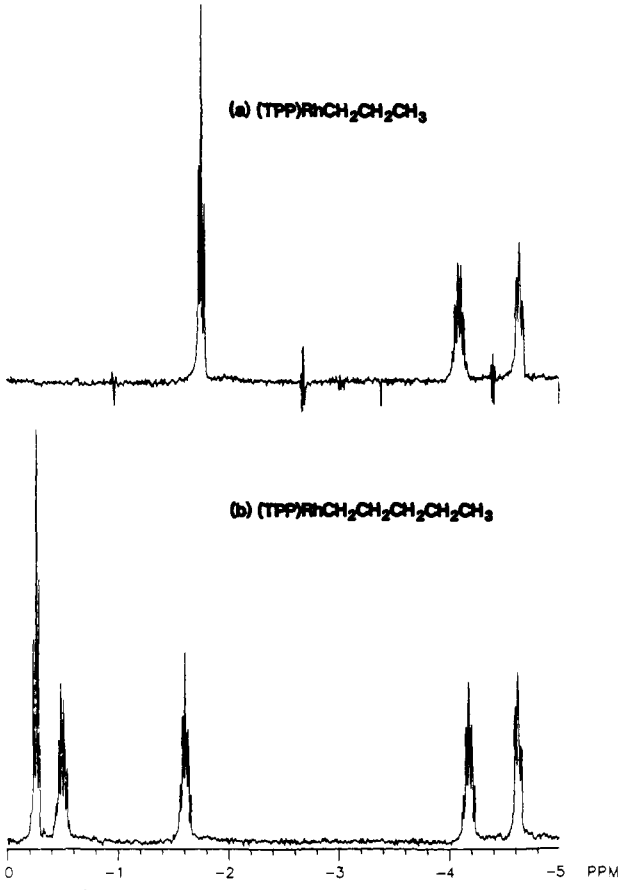

Figure 3. ^{1}H NMR of (TPP)Rh(R) in C_6D_6 from 0.0 to −6.0 ppm for (a) (TPP)Rh(C_3H_7) and (b) (TPP)Rh(C_5H_{11}).

(P)Rh[CHC(X)C_6H_5], X = H, Cl, are known.[3,5,6,12,21-23] However, there are no reports in the literature on the formation of (P)-Rh(C_6H_5) by reaction of (P)Rh or [(P)Rh]$^{-1}$ with C_6H_5X. In contrast, (P)Rh(C_6H_4X) where X = H, OMe, Me, and Cl is formed by reaction of [(P)Rh]$^+$ with C_6H_5X.[24,25] In this case, electrophillic attack on the arene carbon–hydrogen bond by [(P)Rh]$^+$ occurs.

Twelve of the 14 compounds listed in Table I have never been synthesized, and only (TPP)Rh(CH_2Cl)[2] and (TPP)Rh(CH_2I)[26] have been previously reported. The UV–vis spectra of these latter two complexes are similar but not identical with spectra reported in the literature. The differences in the spectra are most likely due to differences in the solvent system. Also, Ogoshi et al.[21] reported the synthesis of a series of (OEP)Rh(CH_2)$_n$$CH_3$ compounds where n = 0–4. Spectroscopic data for these complexes was also reported, but the spectra cannot be directly compared to those in the present study due to the difference between the OEP and the TPP ring systems.

Three different limiting cases describe the kinetics and the thermodynamics of (TPP)Rh(R) formation. The first case includes most of the alkyl halides which were studied and comprises relatively fast reactions between RX and (TPP)Rh. In this case, the homogeneous reaction can be monitored both electrochemically and spectroelectrochemically. The second case comprises complexes where there is a relatively slow reaction between (TPP)Rh and RX. In this case, only the formation of [(TPP)Rh]$_2$ is observed by electrochemistry and spectroelectrochemistry. However,

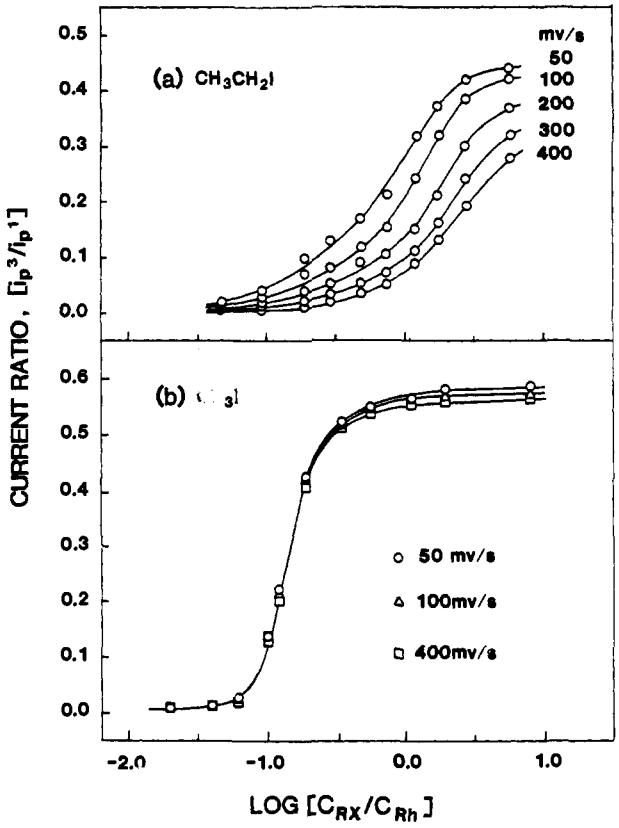

Figure 4. Scan rate dependence on (TPP)Rh(R) formation from (a) CH_3CH_2I and (b) CH_3I. Larger current ratios correspond to increased (TPP)Rh(R) formation.

some (TPP)Rh(R) formation is observed during long time scale spectroelectrochemical experiments. Only the branched alkyl halides belong to this case, and the slow kinetics for the reaction between (TPP)Rh and RX are most likely due to steric hindrance. The third case comprises groups of complexes where there is either no reaction or an extremely slow reaction between (TPP)Rh and RX. In this case, only dimerization of (TPP)Rh is observed. The C_6H_5X aryl halides all belong to this class of compounds.

Reaction Rate Studies. The kinetics for (TPP)Rh(R) formation are complicated by the competing dimerization reaction of (TP-P)Rh. A detailed kinetic study was not possible since neither the concentration of (TPP)Rh nor that of [(TPP)Rh]$_2$ can be accurately monitored throughout the electrochemical titration. However, the relative effect of the alkyl halide on the overall rate constant for (TPP)Rh(R) formation (called k_1) can be monitored.

The effect of both X and the R group on k_1 was determined by a titration of [(TPP)Rh(L)$_2$]$^+$Cl$^-$ with RX, which was monitored by cyclic voltammetry. Cyclic voltammograms of the type shown in Figure 1b were obtained. Plots of i_p^3/i_p^1 vs. log C_{RX}/C_{Rh} were then constructed where i_p^1 and i_p^3 are the peak currents for the first reduction of [(TPP)Rh(L)$_2$]$^+$Cl$^-$ (peak 1, Figure 1) and (TPP)Rh(R) (peak 3, Figure 1). C_{RX} is the concentration of the alkyl halide RX, while C_{Rh} is the concentration of [(TPP)Rh-(L)$_2$]$^+$Cl$^-$.

The ratio of currents for peak 3 and peak 1 gives relative reaction rate data since the current for peak 3 is proportional to the concentration of (TPP)Rh(R) and the concentration of (TPP)Rh produced is directly proportional to the current for peak 1. The peak currents for peaks 1 and 3 are also dependent on the initial concentration of [(TPP)Rh(L)$_2$]$^+$Cl$^-$ and vary with potential scan rate, electrode surface area, and diffusion rates.[27] Thus, the ratio of peak currents and the ratio of concentrations normalizes these experimental factors, and if one assumes that the diffusion coefficients of all porphyrin species are approximately the same, then the ratio i_p^3/i_p^1 can be used to give relative kinetic

(22) Abeysekera, A. M.; Grigg, R.; Trocha-Grimshaw, J.; Viswanatha, V. *J. Chem. Soc., Perkin Trans. 1* **1977**, 1395.
(23) Ogoshi, H.; Setsune, J.; Nanbo, Y.; Yoshida, Z.-I. *J. Organomet. Chem.* **1978**, *159*, 329.
(24) Aoyama, Y.; Yoshida, T.; Sakurai, K.-I.; Ogoshi, H. *J. Chem. Soc., Chem. Commun.* **1983**, 478.
(25) Aoyama, Y.; Yoshida, T.; Sakurai, K.-I.; Ogoshi, H. *Organometallics* **1986**, *5*, 168.
(26) Callot, H. J.; Schaeffer, E. *Nouv. J. Chim.* **1980**, *4*, 311.
(27) Nicholson, R. S.; Shain, I. *Anal. Chem.* **1964**, *36*, 706.

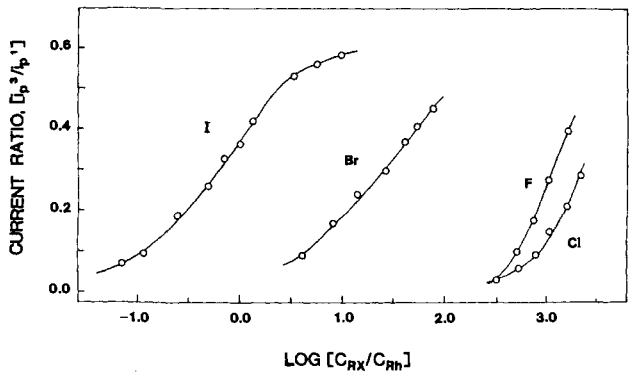

Figure 5. Halide ion dependence on (TPP)Rh($(CH_2)_4CH_3$) formation from $CH_3(CH_2)_4X$ where X = I, Br, Cl, and F. Larger current ratios correspond to increased (TPP)Rh(R) formation. Scan rate = 100 mV/s.

information about the reaction for (TPP)Rh(R) formation.

The scan rate dependence on (TPP)Rh(R) formation is shown in Figure 4. Figure 4a illustrates a plot of i_p^3/i_p^1 vs. log C_{RX}/C_{Rh} for the titration of $[(TPP)Rh(L)_2]^+Cl^-$ with CH_3CH_2I which was monitored at various potential scan rates. As demonstrated in this figure, both the concentration of added CH_3CH_2I and the potential scan rate directly effect the peak current ratio. The ratio of i_p^3/i_p^1 increases as the concentration of CH_3CH_2I is increased. A similar example is shown in Figure 1b. The observed increase in the current ratio as the concentration of RX is increased (Figure 4a) is due to an increase in the rate of reaction of (TPP)Rh with CH_3CH_2I. The increase in current ratio as scan rate is decreased is expected since a decrease in scan rate allows for a more complete formation of (TPP)Rh(CH_2CH_3) before its reduction. This implies that the system is under kinetic control on the time scale of the voltammetric measurements.

The same dependence on scan rate was observed for each of the RX compounds except for CH_3I. Figure 4b shows the plot of i_p^3/i_p^1 vs. log C_{CH_3I}/C_{Rh} at various scan rates. The current ratio is essentially independent of scan rate between 50 and 400 mV/s. This situation indicates that the system is under thermodynamic control. It should be noted, however, that the ratio i_p^3/i_p^1 was never equal to 1.0. This indicates that formation of (TPP)Rh(R) probably does not take place at the electrode surface and that the current for wave 3 involves the diffusion of (TPP)Rh(R) back to the electrode surface.

Figure 5 demonstrates how the halide group of RX effects k_1 at a constant potential scan rate. This figure shows i_p^3/i_p^1 vs. log C_{RX}/C_{Rh} for the series of alkyl halides $CH_3(CH_2)_4X$ where X = I, Br, Cl, and F. In all cases, the reaction is under kinetic control. The product of the reaction is (TPP)Rh($CH_2)_4CH_3$ for all of the halides. However, the C_{RX}/C_{Rh} ratio required to achieve a specific current ratio follows the trend I < Br < F ≤ Cl. This implies that k_1 follows the trend I > Br > F ≥ Cl for $CH_3(CH_2)_4X$. The difference between F and Cl is relatively small and may not be significant. This same general trend was observed for each of the RX compounds studied. This effect of X on the reactivity of RX is well-known and can be attributed to an increase in R–X bond strength as X changes from I to F.[28]

Figure 6 shows how the R group of RX effects k_1. This figure plots i_p^3/i_p^1 vs. log C_{RX}/C_{Rh} for a series of $CH_3(CH_2)_nI$ compounds where n = 0–4. The products in this case are (TPP)Rh-($CH_2)_nCH_3$, where n = 0–4. The reaction is under kinetic control with the exception of CH_3I as a reactant. In this case the reaction is under thermodynamic control. As seen in this figure, a specific current ratio can be reached at a much lower concentration of CH_3I (n = 0) then for any of the other $CH_3(CH_2)_nI$ compounds. Hence, one can conclude that k_1 is much larger for CH_3I than that of the other alkyl halides. This was also observed to be the case for the other RX compounds and is related to the size of the alkyl halide. The importance of alkyl halide size is dramatically demonstrated by complexes where the carbon chain is branched.

(28) Kerr, J. A. *Chem. Rev.* **1966**, *66*, 465.

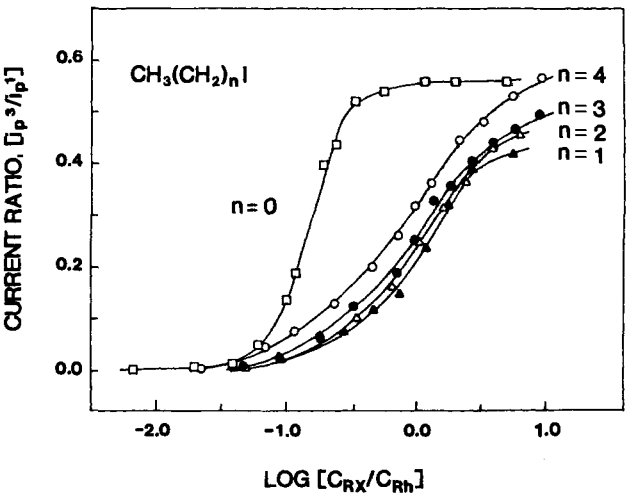

Figure 6. Alkyl chain length dependence on (TPP)Rh($(CH_2)_nCH_3$) formation from $CH_3(CH_2)_nI$ at a scan rate of 100 mV/s. Larger current ratios correspond to increased (TPP)Rh(R) formation.

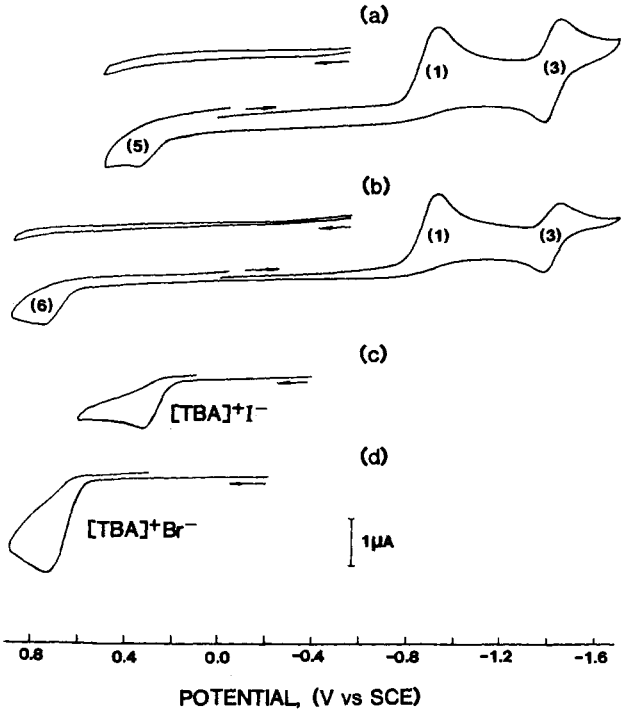

Figure 7. Cyclic voltammogram for (a) 4.6 × 10^{-4} M $[(TPP)Rh(L)_2]^+Cl^-$ in the presence of 12 equiv of 1-iodopropane, (b) 4.0 × 10^{-4} M $[(TPP)Rh(L)_2]^+Cl^-$ in the presence of 400 equiv of 1-bromopropane, (c) 2 × 10^{-3} M TBAI, and (d) 1.9 × 10^{-3} M TBABr. All voltammograms in 0.2 M TBAP/THF solution. Scan rate = 100 mV/s.

For these alkyl halides no reaction was electrochemically detectable, and a homogeneous reaction could only be observed by spectroelectrochemistry on long time scales.

The value of C_{RX}/C_{Rh} necessary to reach a specific current ratio is about the same for $CH_3(CH_2)_nI$, n = 1–4 (see Figure 6). Hence, values of k_1 for these complexes are about equal. This suggests that straight chain alkyl halides with two or more carbons have about equal steric hindrance. It is interesting to note that $CH_3(CH_2)_nX$ complexes with $n \geq 1$ have a k_1 which appears to increase for increased values of n.

Mechanism for the Reaction of (TPP)Rh with RX. The formation of both X^- and (TPP)Rh(R) from (TPP)Rh and RX can be demonstrated by electrochemical techniques. The method of X^- formation is important for mechanistic considerations. Figure 7a shows the cyclic voltammograms of $[(TPP)Rh(L)_2]^+Cl^-$ in the presence of 12 equiv of 1-iodopropane while Figure 7b shows the cyclic voltammogram of $[(TPP)Rh(L)_2]^+Cl^-$ in the presence of

400 equiv of 1-bromopropane. Before scanning in a negative direction, no oxidation waves are observed up to +0.9 V, which is the anodic limit of the solvent. However, after negatively scanning past the first reduction of $[(TPP)Rh(L)_2]^+Cl^-$ (wave 1), a new oxidation wave is observed at +0.34 V for 1-iodopropane (wave 5, Figure 7a) and at +0.73 V for 1-bromopropane (wave 6, Figure 7b). $(TPP)Rh(C_5H_{11})$ is formed in both cases and is not oxidized until potentials more positive than +1.0 V. Similar cyclic voltammetric results were obtained with all of the RI and RBr compounds which showed reactivity (see Table I). Cyclic voltammetric experiments show that tetrabutylammonium iodide (TBAI) and tetrabutylammonium bromide (TBABr) are irreversibly oxidized at +0.34 and +0.73 V, respectively (see Figure 7c,d). Thus the wave at +0.34 V in Figure 7a is assigned as the oxidation of I^- and the wave at +0.73 V in Figure 7b as the oxidation of Br^-. These potentials agree with potentials given in previous reports[29] for the oxidation of I^- and Br^-.

Integration of the total current for the first reduction peak of $[(TPP)Rh(L)_2]^+Cl^-$ in the presence of RX gives coulometric values of n that are dependent upon RX. When X = Cl, $n = 1.0 \pm 0.1$ electron per Rh atom. In contrast, when X = Br and I, $n = 1.3 \pm 0.1$ and 1.5 ± 0.1 electron per Rh atom, respectively. Formation of (TPP)Rh(R) and Cl^- from $[(TPP)Rh(L)_2]^+$ and RCl requires a total of two electrons, and this is not experimentally observed. Thus the overall reaction for formation of (TPP)Rh(R) can best be described by equations 1-3, where S is an electron source other than the electrode.

$$[(TPP)Rh(L)_2]^+ \xrightarrow{e} (TPP)Rh + 2L \quad (1)$$

$$(TPP)Rh + RX \rightarrow (TPP)Rh(R) + X^\bullet \quad (2a)$$

$$(TPP)Rh + RX \rightarrow [(TPP)Rh(R)]^+ + X^- \quad (2b)$$

$$X^\bullet + S \rightarrow X^- + S^+ \quad (3a)$$

$$[(TPP)Rh(R)]^+ + S \rightarrow (TPP)Rh(R) + S^+ \quad (3b)$$

After generation of (TPP)Rh and attack at the R-X bond, either loss of $X^\bullet$ and formation of (TPP)Rh(R) (eq 2a) or loss of X^- and formation of $[(TPP)Rh(R)]^+$ (eq 2b) will occur. Reaction pathways 2a and 3a will be followed when X = Br and I. In this case $X^\bullet$ formation can occur if one considers that the potential for the $(TPP)Rh(R)/[(TPP)Rh(R)]^+$ couple is near +1.0 V in benzonitrile,[30] while the $X^-/X^\bullet$ potential is less than +1.0 V. On the other hand, path 2b and 3b will be followed when X = Cl or F. The $X^-/X^\bullet$ potential of chloride and fluoride is greater than 1.0 V, and reaction paths 2a and 3a will not occur. However, in the case of X = Br and I, some electrochemical reduction of $X^\bullet$ to X^- is observed thus accounting for the increase in coulometric value of n. Apparently, some $I^\bullet$ and $Br^\bullet$ have time to diffuse back to the electrode surface after the chemical reaction between RX and (TPP)Rh. It should be noted that a careful measurement of the background current was performed in the presence of RX and the possibility that the increase in n for X = Br and X = I was due to direct reduction of RX was eliminated.

Formation of (TPP)RhX is not observed in any of the electrochemical or spectroelectrochemical experiments. For example, (TPP)RhCl is reduced at -1.2 V in benzonitrile,[30] and the generation of this species would be observed by the cyclic voltammograms. This lack of (TPP)RhX generation is in contrast to reports that the reaction of $[(P)Rh]_2$ with RX gives (P)Rh(X).[3,5,12]

A mechanism has been previously proposed for the reaction of $[(OEP)Rh]_2$ with RX.[12] (OEP)Rh is proposed to react with RX to form (P)Rh(X) and $R^\bullet$ after dissociation of the dimer. The $R^\bullet$ radical then combines with another $[(OEP)Rh]_2$ unit to form (OEP)Rh(R). The data presented in this paper clearly suggests an alternate pathway for the reaction of (TPP)Rh and RX as indicated by eq 1-3. The effects of R and X on the overall rate constant are consistent with this type of reaction pathway and not with $R^\bullet$ formation. However, the observation of different reaction pathways and different products in these two studies can be rationalized if one considers the relative stabilities of $R^\bullet$. In the present case, formation of $R^\bullet$ would result in generation of a radical such as $CH_3^\bullet$ or $(C_nH_{2n+1})^\bullet$. In the previous study formation of $C_6H_5CH_2^\bullet$ was proposed, which is considerably more stable.[28] Hence, in the latter case a radical pathway may predominate.

Acknowledgment. The support of the National Science Foundation (Grant No. CHE-8515411) is gratefully acknowledged.

(29) Bard, A. J.; Merz, A. *J. Am. Chem. Soc.* **1979**, *101*, 2959.

(30) Unpublished data.

A Comparison of Electron Donor and Proton Abstraction Activities of Thermally Activated Pure Magnesium Oxide and Doped Magnesium Oxides

Kenneth J. Klabunde* and Hiromi Matsuhashi

Contribution from the Department of Chemistry, Kansas State University, Manhattan, Kansas 66506. *Received June 30, 1986*

Abstract: Thermal activation of microcrystalline MgO at 400-700 °C has been carried out under vacuum and under rapid flows of N_2, Ar, O_2, and H_2/N_2. Some samples of MgO were impregnated or coprecipitated with LiOH, NaOH, or $Al(OH)_3$ before activation. The activities for 1-butene isomerization, where proton abstraction is rate limiting, were compared with activities for CO telomerization/reduction, where electron donation capability is most important. These studies suggest that defect sites are involved and that localized electron rich domains can be enhanced by Li^+ substitution for Mg^{2+} but that localized more electron difficient domains can be enhanced by Al^{3+} substitution for Mg^{2+}. These studies also show that high-temperature thermal activation with gas flow of N_2 or Ar is possible, but that O_2 and H_2/N_2 anneal out defects and activity is lost.

The remarkable properties of thermally activated polycrystalline MgO are well-documented.[1] To illustrate this consider the following: (1) catalysis of $H_2 + D_2 \rightarrow 2HD$, $E_a \sim 2$ kcal/mol which is considerably lower than the gas-phase E_a for $H^\bullet + D_2$

0002-7863/87/1509-1111$01.50/0